Available on the CERN CDS information server **CMS PAS BPH-08-004**

CMS Physics Analysis Summary

Contact: cms-pag-conveners-bphysics@cern.ch 2009/08/08

Measurement of the Azimuthal Correlation in $b\bar{b}$ Production in pp Collisions with the CMS detector

The CMS Collaboration

Abstract

We present an analysis aimed at the measurement of the azimuthal angular correlation of $b\bar{b}$ production. We use $b\bar{b} \to (J/\psi X)(\ell X')$ events, where the charged lepton is a muon, to measure the azimuthal opening angle $\Delta\phi$ between the bottom quarks. The $b\bar{b}$ purity is determined as a function of $\Delta\phi$ by a simultaneous fit to the J/ψ invariant mass and decay length, and the lepton impact parameter.

1 Introduction

The dominant b-quark prodution mechanism at the Large Hadron Collider (LHC) is believed to be pair production through the strong interaction. Predictions from next-to-leading-order (NLO) perturbative QCD [1] have historically underestimated both the observed inclusive b and correlated $b\bar{b}$ production cross section at the Tevatron [2]. Possible explanations for the disagreement between the measured and predicted cross-sections include b fragmentation models [3], higher-order $b\bar{b}$ production mechanisms [4], and, speculatively, supersymmetric production mechanisms [5]. In addition, a recent analysis [6] by the CDF collaboration has observed a significant previously unidentified background due to long-lived muon sources, which could account for the discrepancy between data and theory in analyses relying on muons to identify b hadrons. New data from the LHC will be a critical additional test of NLO QCD and its ability to predict accurately the expected background rates in searches for Standard Model processes (e.g., top production) and new particles (Higgs, SUSY, etc).

The study of $b\bar{b}$ correlations is an important test of the effective contributions from higher-order QCD processes to the b-quark production that can be performed with the very first data collected by CMS. The QCD production mechanisms are usually divided in the following categories:

- Flavor Creation (FC): it refers to the lowest order two-to-two QCD $b\bar{b}$ production diagrams. This process includes $b\bar{b}$ production through $q\bar{q}$ annihilations and gluon fusion, plus higher-order corrections to these processes. Because this production is dominated by two-body final states, it tends to yield $b\bar{b}$ pairs that are back-to-back in $\Delta\phi$ and balanced in p_T.
- Flavor Excitation (FE): it refers to diagrams in which a $b\bar{b}$ from the quark sea of the proton is excited into the final state because one of the quarks from the $b\bar{b}$ pair undergoes a hard QCD interaction with a parton from the other beam particle. Because only one of the quarks in the $b\bar{b}$ pair undergoes the hard scatter, this production mechanism tends to produce b quarks with asymmetric p_T.
- Gluon Splitting (GS): it refers to diagrams where the $b\bar{b}$ pair arises from a $g \rightarrow b\bar{b}$ splitting in the initial or final state. Neither of the quarks from the $b\bar{b}$ pair participates in the hard QCD scatter. Depending on the experimental range of b quark p_T sensitivity, gluon splitting production can yield a $b\bar{b}$ distribution with a peak at small $\Delta\phi$.

Previous measurements of azimuthal correlation distributions at the Tevatron generally agree with the shape predicted by NLO calculations, but not in the normalization [2]. Measurements of $b\bar{b}$ production at the LHC will provide a fundamental test of the QCD predictions in a new energy regime and with much higher statistics. The first step in this effort will be to measure the total $b\bar{b}$ cross section and the differential cross section $d\sigma/d\Delta\phi$ with respect to the opening angle between the two b quarks, and this document describes the sensitivity CMS can expect in the first 50 pb^{-1} of collision data. The longer-term goal will be to use the measured cross section to "tune" Monte Carlo generators to more accurately reproduce the observed data, and thereby obtain more realistic estimates of background rates in searches for new particles that decay to bottom quarks.

2 Analysis Strategy

The goal of this analysis is a measurement of $b\bar{b}$ correlations ($d\sigma/d\Delta\phi$) with the CMS detector using early data. The presence of b-quark decays is detected entirely through muonic signatures. The decay of one b is tagged by reconstructing the decay $J/\psi \to \mu^+\mu^-$. Events are also required to contain an additional muon consistent with the semileptonic decay of the second b. This approach is characterized by lower yields with respect to b-quark identification through jet signatures, but it retains the highest sensitivity for $b\bar{b}$ production at small opening angles where NLO processes dominate. We measure the yield in each of eight $\Delta\phi$ intervals using a simultaneous unbinned maximum-likelihood fit to the J/ψ invariant mass, the transverse flight length L_{xy} of the J/ψ, defined as the distance in the x-y plane between the primary vertex and the common vertex of the J/ψ dimuon pair, and the impact parameter d_{xy} of the third muon in the event. Since the size of each $\Delta\phi$ bin is comparable to the measured resolution, an unfolding procedure is necessary to correct the reconstructed $\Delta\phi$ distribution back to the original b quarks. The final sample is expected to be characterized by low backgrounds, and is ideal for early data analysis since we do not rely at all on jets or complicated b-tagging algorithms. In addition, this analysis will be able to provide useful inputs to the detector commissioning regarding the muon reconstruction and identification (in particular on the low p_T region of the spectrum), the trigger efficiency, and the tracker alignment. In this feasibility study we assume $\sqrt{s} = 10\,\text{TeV}$ and $\mathcal{L} = 50\,\text{pb}^{-1}$, unless specified otherwise.

3 Monte Carlo Samples

The selection criteria and the fit technique are optimized using an inclusive sample of 1.2×10^6 $pp \to b\bar{b} \to J/\psi X$ events, corresponding to an integrated luminosity of about 50 pb^{-1}. An additional independent sample of the same size is used to validate the fit technique. Event generation and b hadronization are performed with PYTHIA [1], while the b hadron decays are generated using EvtGen [8]. One of the two b quarks in the event is required to hadronize into a bottom hadron decaying to $J/\psi X$, including cascade decays initiated by higher-mass charmonium states. Generated events are required to include two muons generated with $p_T > 2.5\,\text{GeV}/c$ and $|\eta| < 2.5$. Because the second b quark in the event does not have any particular constraint on its decay modes, the inclusive $b \to J/\psi X$ sample also allows to perform studies on background from $b\bar{b}$ events. Background from prompt J/ψ is studied with a dedicated sample of 1.8×10^6 inclusive $pp \to J/\psi\, X$ events, corresponding to an integrated luminosity of about 16 pb^{-1}, where the J/ψ is forced to decay in the dimuon channel. In addition, we use an inclusive sample of 5.2×10^6 mimimum bias Pythia $pp \to \mu X$ events (about 0.04 pb^{-1}), with at least one muon required at the generator level, to cross-check our background estimates.

4 Trigger

Due to the clean signature of the final state under analysis, a loose muon High Level Trigger (HLT) provides a reasonable selection efficiency without significantly increasing the non-$b\bar{b}$ backgrounds. We use a dimuon trigger [9]. The total dimuon trigger efficiency is found to to be $\epsilon_{\text{trg}} = 0.218$ using the inclusive $b \to J/\psi\, X$ sample. The double-muon trigger efficiency as a function of true J/ψ p_T is shown in Fig. 1, where we define the trigger efficiency as:

[1] We use PYTHIA [7] version 6.416 and the PDF library CTEQL61.

$$\epsilon_{J/\psi}(p_T) = \frac{N_{\rm trg}(p_T^{J/\psi})}{N^{\rm gen+filter}(p_T^{J/\psi})}. \quad (1)$$

Here $N_{\rm trg}$ is the number of events passing the trigger, and $N_{\rm gen+filter}$ is the number of events passing the generator-level muon filter. The dip in the low p_T region is due to kinematic effects, since muon pairs near the trigger threshold have a larger probability to pass the threshold when the J/ψ is moving along the beam axis, than when the J/ψ has a small transverse boost. The dimuon trigger consists of a Level1 (L1) trigger, based on the muon chamber information, followed by the HLT step, that confirms the L1 and refines the reconstruction adding the silicon tracker information (Level 3). It requires two Level 3 muon with $p_T > 3$ GeV/c. The distance in the transverse plane between the Level 3 muons and the beam spot was required to be less than 2 cm.

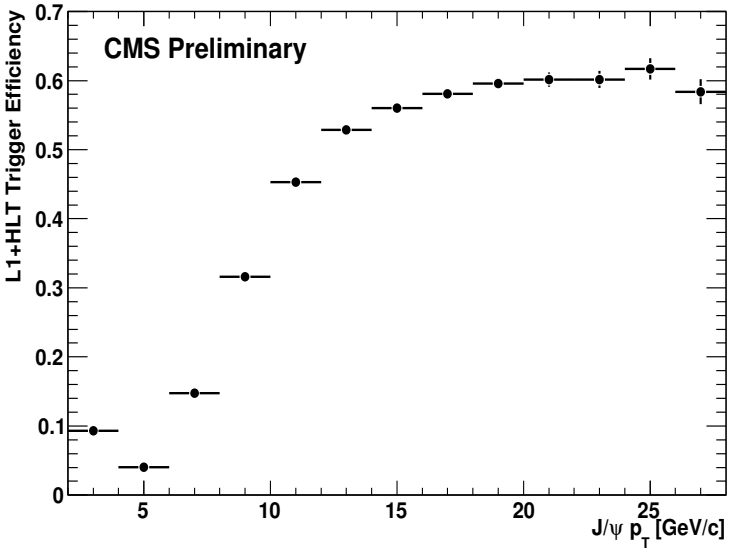

Figure 1: Trigger Efficiency in signal events for the double-muon trigger as a function of the true J/ψ transverse momentum.

5 Event Reconstruction

The event reconstruction starts by building J/ψ candidates by vertexing every pair of muon candidates with opposite electric charge using the Kalman filter formalism. We require the vertexing to be successful and we select the best J/ψ candidate event by event as the one with the highest vertex probability. We then require a third muon in the event; in case of more than one reconstructed additional muon candidate, we select the one with the highest p_T. We require all three muons in the event to have $p_T > 3$ GeV/c and $|\eta| < 2.4$. To increase the purity of the third muon we apply additional selection criteria on the quality of the silicon tracker fit (at least 11 silicon tracker hits and the track fit χ^2/NDOF < 1.9), calorimeter deposited energy, and the penetration depth in the muon system. We estimate an effective cross-section for $J/\psi + \mu$ decays of about 145 pb. The resulting J/ψ invariant mass distribution after all the selection criteria is shown in Fig. 2, and, in logaritmic scale, in Fig. 9 in Appendix.

We identify four different components in the reconstructed sample:

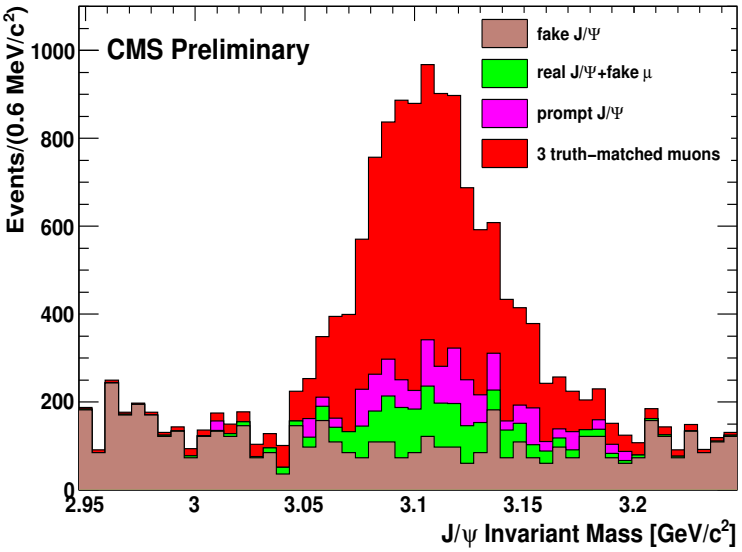

Figure 2: J/ψ invariant mass distribution after all the selection criteria. The different truth-matched components are stacked and shown in different colors.

- **Signal**: events with a correctly identified J/ψ and a correctly identified third muon. This muon comes from semileptonic decays of the second bottom hadron in the event, cascade decays ($b \to cX \to \ell X'$), τ decays ($b \to \tau X \to \mu X'$) or from a second $b \to J/\psi X$ decay (which occurs in about 1% of all signal events).
- **Fake Muon**: events with a correctly identified J/ψ and a misidentified muon. In principle this particle could be a hadron misidentified as a muon (e.g. punch-through hadrons) or real muons from pion or kaon decays-in-flight (DIF).
- **Prompt** J/ψ: events with a correctly identified J/ψ that comes from the primary vertex. We estimate an effective cross-section for these decays of about 25 pb.
- **Fake** J/ψ: events with a fake J/ψ candidate, where one or both the muons are not coming from the J/ψ decay. These events have a flat J/ψ invariant mass distribution and are mainly composed of events with one correctly identified muon from the J/ψ decay, and a second muon from the rest of the event. In $b\bar{b}$ events where the second μ comes from the second b, the two b quarks have $\Delta\phi$ near zero. This effect can be seen in Fig. 3, where we show the $\Delta\phi$ distributions after all the selection criteria have been applied.

In Fig. 4 we show the impact parameter distributions for decay-in-flight muons compared with the corresponding distribution for muons from bottom and cascade decays, and fake μ from hadronic punch-through. The impact parameter shapes for the two background sources are in good agreement within the statistics currently available. Therefore, in the signal yield fit we use the same impact parameter Probability Density Function (PDF) for hadronic punch-through and decays-in-flight.

There is also an irreducible background coming from $B_c \to J/\psi\,\mu X$. Semileptonic B_c decays are present in the inclusive $b \to J/\psi X$ sample with a branching fraction of about $\mathcal{B}(b \to B_c) \cdot \mathcal{B}(B_c \to J/\psi\mu X) = (2.7 \pm 0.3) \times 10^{-5}$, in good agreement with the PDG value $(5.2^{+2.4}_{-2.1}) \times 10^{-5}$ [10]. No B_c semileptonic decay passes the selection criteria in the inclusive $b \to J/\psi X$

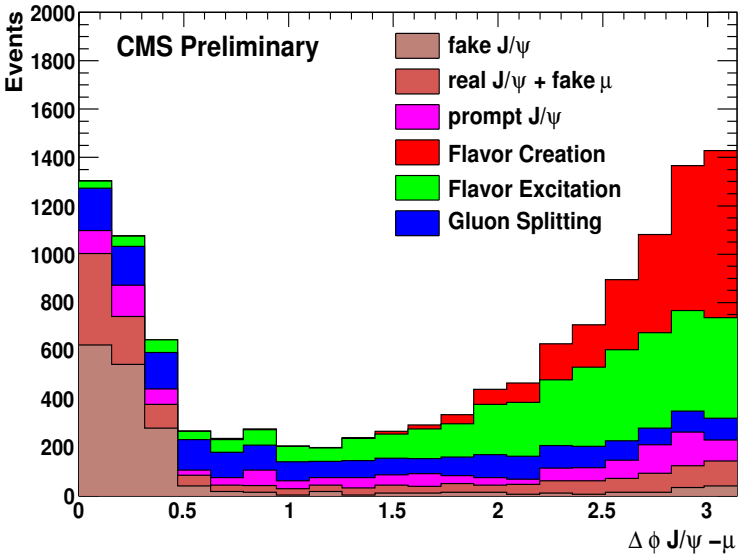

Figure 3: $J/\psi - \mu$ $\Delta\phi$ distribution after all the selection criteria. The different truth-matched components are stacked and shown in different colors.

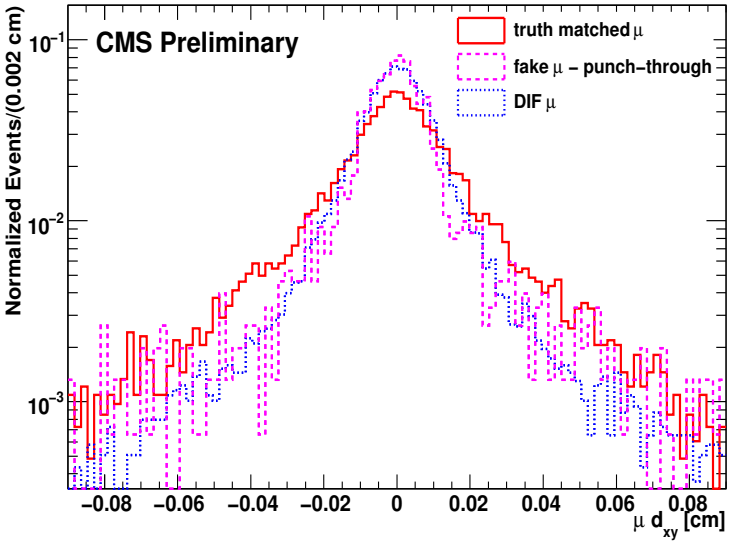

Figure 4: Impact parameter distributions for muons from bottom and cascade decays (red-solid), fake muons from hadronic punch-through (magenta-dashed), and DIF muons (blue-dotted). All the distributions are normalized to unit area.

sample, from which we can estimate an effective cross-section for these decays of about 1 pb.

6 Signal Extraction

The $b\bar{b}$ yield in the different $\Delta\phi$ intervals is obtained by a simultaneous, unbinned maximum-likelihood fit to the dimuon invariant mass $M_{\mu\mu}$, transverse flight length L_{xy}, and the impact

parameter d_{xy} of the third muon. As the J/ψ and the additional muon originate from separate bottom hadron decays, L_{xy} and d_{xy} are not strongly correlated for signal events. J/ψ candidates are assumed to originate from three sources: direct J/ψ production (including feed-down from χ_{c1}, χ_{c2} and $\psi(2s)$) where the J/ψ decays at the primary vertex, non-prompt J/ψ from bottom decays, and the fake combinatorial background described by the events in the $M_{\mu\mu}$ sidebands. Candidates for the third muon are assumed to originate from the following sources: directly produced fake or real muons from the primary vertex, muons from bottom decays (including cascade decays from $b \to cX \to \ell X'$), and real or fake muons combined with a fake J/ψ candidate.

The backgrounds in this analysis have two categories: one in which L_{xy} and d_{xy} are correlated, and the other where they are uncorrelated. These variables are correlated for events where both the J/ψ and the additional muon candidates originate from the same displaced vertex. We find that neglecting this correlation doesn't introduce any sizable bias. Only one component is used to model prompt J/ψ decays, including both cases in which the third muon is real or fake. We adopt this choice due to the small effective cross-section for this component, and the high discriminating power given by the J/ψ transverse flight length to identify prompt J/ψ decays.

The PDFs used in the fit to the J/ψ and μ distributions are built using the Monte Carlo signal sample, as described in Sec. 3. The following analytical functions are used to build the PDFs:

- $\boldsymbol{M_{\mu\mu}}$: we use a sum of three Gaussians. The additional Gaussians are required to account for the pseudorapidity dependence of the dimuon mass and resolution.
- $\boldsymbol{L_{xy}}$: for the non-prompt J/ψ component we use an exponential convolved with two Gaussians, where the second Gaussian is needed to account for outliers (few %) at large values of L_{xy}. For the prompt J/ψ transverse flight length PDF, we use a double-tail exponential function. The resolution of the core Gaussian function is computed event-by-event using the measured error on the flight length.
- $\boldsymbol{d_{xy}}$: we use an exponential convolved with two Gaussians to describe both the prompt and non-prompt samples (with different effective lifetimes, of course). The resolution of the core Gaussian function is computed event-by-event using the measured error on the impact parameter. As in the case of L_{xy}, the second Gaussian function accounts for outliers at large values of $|d_{xy}|$.

Figure 5 shows the fit results for a typical sample, corresponding to an integrated luminosity of about 13 pb^{-1}. We validate the fit procedure using a large sample of pseudoexperiments, and by fitting multiple samples of statistically independent fully simulated events, such as the sample in Fig. 5.

7 Unfolding of the $\Delta\phi$ Distribution

The measured spectrum of a physical observable, like the $J/\psi - \mu$ azimuthal correlation, is usually distorted by detector effects, such as the limited acceptance. Moreover, in our analysis the chosen $\Delta\phi$ bin size is comparable to the resolution (mainly limited by the use of $b \to \mu X$ to tag one of the b in the event), so there is a significant migration of events generated in one bin of $\Delta\phi(b\bar{b})$ and ending up in a different bin of reconstructed $\Delta\phi$ between the J/ψ and muon candidates. A comparison of the measured spectrum with that predicted by theory requires that we remove these effects to obtain the true underlying physical spectrum. We use the technique described in Ref. [11], based on singular value decomposition of the detector response matrix, shown in Fig. 6.

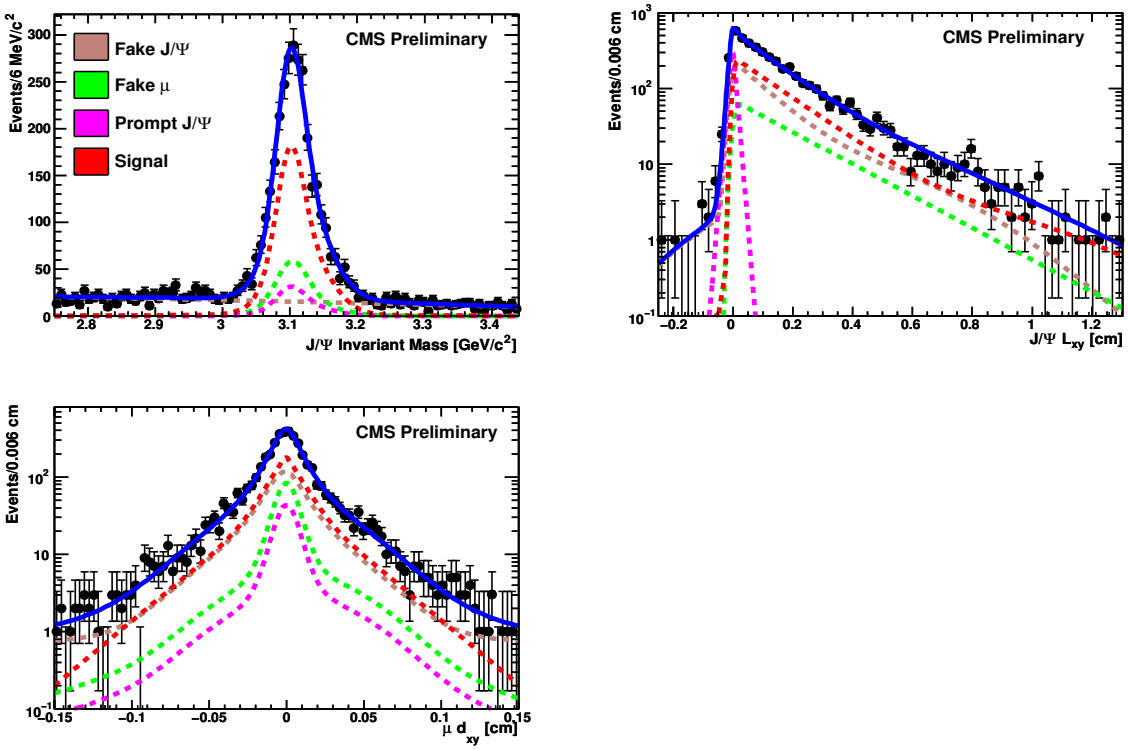

Figure 5: Results of the three-dimensional fit for a typical Monte Carlo sample. The Monte Carlo distributions (points with error bars) are compared to the results of the overall fit (solid line, blue color). The PDFs for the different fit components are shown in different colors.

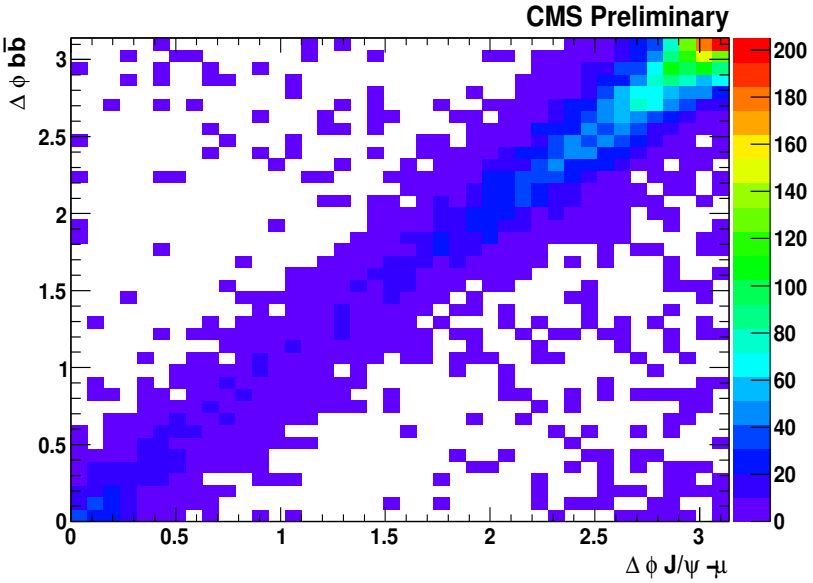

Figure 6: Detector response matrix showing the reconstructed $\Delta\phi_{J/\psi-\mu}$ as a function of the generated $\Delta\phi_{b\bar{b}}$ obtained on simulated signal events.

In order to suppress spurious oscillations originating from statistical fluctuations in the data, the unfolding procedure includes a regularization term. The regularization term depends on one parameter, usually indicated as τ, and the determination of τ is of crucial importance in the unfolding process. Choosing a small value for τ will bias the result towards the simulation input. On the other hand, an insufficient damping (large τ) will lead to a result substantially influenced by statistical fluctuations in the measured spectrum. The value of τ can be chosen as any integer between a minimum value of 1 ("the solution corresponds to the true simulated distribution") and a maximum value equal to the number of bins in the histogram to be unfolded ("no regularization"). We choose the value of τ by minimizing the bias in a set of toy tests where the "measured" distribution is unfolded and the result is compared to the original "true" distribution for all possible values of τ. The bias is defined as the χ^2 between the unfolded and the generated distributions for the entire ensemble of toys. The toy tests are performed using statistically independent toy MC samples for the initialization and for the distributions to be unfolded. For each test, the first MC sample serves to determine the detector response matrix and the initial generated MC distribution. The reconstructed distribution, instead of a truly measured distribution from data, is taken from a second, statistically independent, MC sample, where the different production mechanism contributions are varied by $\pm 20\%$. The bias obtained from a Gaussian fit to the pull distributions in each $\Delta\phi$ bin is used to estimate the systematic uncertainty intrinsic in the unfolding procedure. In Fig. 7 we show the comparison between the generated and unfolded $\Delta\phi$ distributions, using the regularization parameter $\tau = 6$.

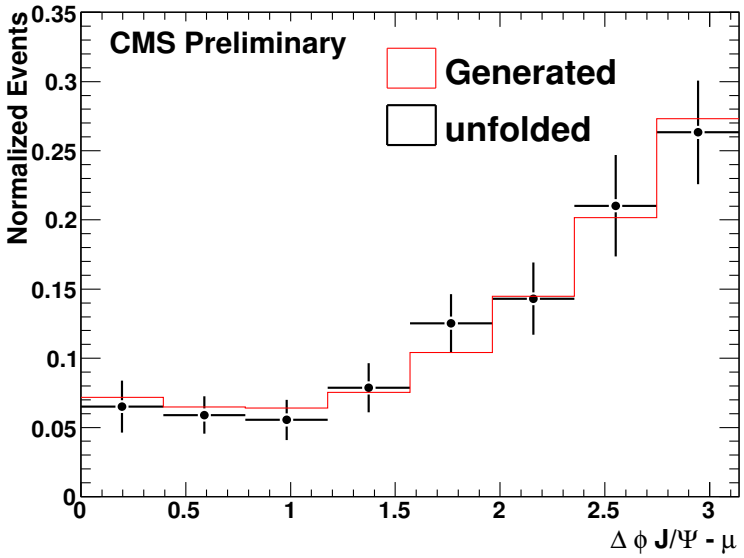

Figure 7: Comparison of the reconstructed and unfolded (black with error bars) and generated (red histogram) distributions of $\Delta\phi$. The distributions are normalized to unit area.

8 Systematic Uncertainties

Several different sources of systematic uncertainty have been considered, and a summary is reported in Table 1. Apart from the fit and unfolding biases that must be estimated with Monte Carlo studies, the remaining systematic uncertainties can be estimated directly on data. Truth-matched muons from the second b-quark decay in the event may come directly from the b

(semileptonic decays of B, B_s or bottom baryons, or from a second J/ψ in the event) or may come from charm semileptonic decays (cascade decays, $b \to cX \to \ell X'$). The uncertainty on the relative rate of the two contributions has to be considered a source of systematic uncertainty, because a muon from cascade decays will have a larger impact parameter than muons from b decay. We modify the relative rate of direct bottom hadron and cascade decays by 20% and we repeat the fit using the modified PDF shape for the muon impact parameter. The difference in the yield in each $\Delta\phi$ bin between the nominal fit and the one with the modified PDF shape is taken as systematic uncertainty. The bottom hadron lifetimes (B^+, B^0, B_s and Λ_b) and the impact parameters of their decay products are strongly correlated. B_s, B^+, B^0 and Λ_b have proper decay lengths varying between about 490 μm (B^+) and 415 μm (Λ_b). Thus the uncertainty in the fraction of bottom quarks fragmenting to the different bottom hadrons, and in particular to Λ_b, leads to a systematic uncertainty on the impact parameter and J/ψ flight-length PDFs. We modify the relative rate of the B^+, B^0, B_s and Λ_b bottom hadrons by the corresponding errors listed in the PDG [10], and we repeat the fit using the modified PDF shapes for the J/ψ transverse flight length and muon impact parameter. The largest difference in the yield in each $\Delta\phi$ bin between the nominal fit and the one with the modified PDF shapes is taken as systematic uncertainty. For the systematic uncertainty due to the PDF shapes, a toy MC approach is used in which we perform an ensemble of fits: the PDF parameters (fixed from the MC signal fits) are varied within their uncertainties for N "experiments" and the fit is repeated with the new set of PDF parameters. The RMS spread in the resulting signal yield distributions for the N experiments in each $\Delta\phi$ bin is taken as systematic uncertainty. Intrinsic biases due to the fit technique and the unfolding method are estimated using toy Monte Carlo fits, as described in the above section. We include a systematic uncertainty due to the finite Monte Carlo statistics and due to the background from semileptonic $B_c \to J/\psi\mu X$ decays.

We include a systematic uncertainty due to the J/ψ polarization and residual misalignment. The J/ψ reconstruction efficiency depends on the J/ψ polarization, and therefore affects the reconstruction efficiency in the different $\Delta\phi$ bins. A systematic uncertainty is evaluated by shifting the polarization measured by CDF [12] (for prompt J/ψ's) and BaBar [13] (for non-prompt J/ψ) by 3σ, a conservative but justified shift given the inconsistencies between CDF Run 1 and Run 2 measurements. Uncertainties from misalignment in early data have been assessed by comparing different misalignment scenarios. Tag and probe methods will be used to assess the systematic uncertainties on the reconstruction and trigger efficiencies coming from a non-perfect detector Monte Carlo simulation. Dedicated study groups will assess this uncertainty for CMS.

For the absolute cross section measurement we also need an estimate of the luminosity. The expected uncertainty on the luminosity measurement in the early running is 10%. Since this is the largest single systematic uncertainty thus far evaluated, it would also be possible to measure the azimuthal correlation relative rate with respect to the peak bin at π, which would remove all of the systematic sources that are common between $\Delta\phi$ bins, while retaining the fundamental information in the shape of the distribution.

9 Results and Conclusions

In summary, due to the large $pp \to b\bar{b}$ cross-section at the LHC energies, CMS will be able to measure properties of b-quark production and $b\bar{b}$ correlations and test NLO QCD predictions using early data. The goal of this analysis is a measurement of the $b\bar{b}$ azimuthal correlation differential cross-section $d\sigma/d\Delta\phi$, obtained using a clean fully leptonic signature. Figure 8 shows the final differential cross section measurement as determined on a Monte Carlo sample corre-

Source	Bin 1	Bin 2	Bin 3	Bin 4	Bin 5	Bin 6	Bin 7	Bin 8
	Relative Error (in %)							
cascade decay rate	1.1	0.7	1.2	1.	0.4	1.2	0.7	1.
bottom hadron rate								
$J/\psi L_{xy}$	4.8	2.6	4.1	2.6	2.6	0.9	1.8	0.7
μ IP	3.7	2.9	0.6	1.5	1.8	2.2	1.9	2.6
PDF shape								
J/ψ invariant mass	0.7	0.4	0.4	0.1	0.1	0.2	0.2	0.1
$J/\psi L_{xy}$	2.8	1.9	0.3	1.1	0.9	0.7	0.4	0.7
μ IP	7.6	4.4	5.	4.5	3.3	3.6	2.8	3.
Fit Bias	0.7	0.5	1.4	0.3	0.3	0.1	0.1	0.2
Unfolding Bias	1.1	0.02	0.2	5.8	3.1	2.4	0.3	1.2
$B_c \to J/\psi\mu X$	3.5	1.5	-	-	-	-	-	-
Trigger/Muon Efficiency	5.	5.	5.	5.	5.	5.	5.	5.
MC Statistics	3.2	3.4	3.6	3.5	2.9	2.1	1.7	1.3
J/ψ Polarization	4.3	4.3	4.2	4.3	4.3	4.3	4.2	4.3
Misalignment	2.4	2.4	2.4	2.4	2.4	2.4	2.4	2.4
Luminosity	10	10	10	10	10	10	10	10
Total	16.7	14.2	14.4	15.1	13.8	13.4	12.9	13.

Table 1: Summary of the different sources of systematic uncertainty. The columns are labeled by $\Delta\phi$ bin from the lowest to the highest value.

sponding to $50\,\mathrm{pb}^{-1}$. The unfolding procedure has been applied, and the final cross section per $\Delta\phi$ bin is calculated according to the following equation:

$$\frac{d\sigma}{d\Delta\phi} = \frac{N_{\mathrm{fit}}}{\mathcal{L}\cdot\epsilon_{\mathrm{trg}}\cdot\epsilon_{\mathrm{reco}}}, \tag{2}$$

where N_{fit} is the fitted signal yield in a given bin after applying the unfolding procedure, $\mathcal{L}$ is the integrated luminosity, ϵ_{trg} is the trigger efficiency for the dimuon trigger, and ϵ_{reco} is the total reconstruction efficiency for the J/ψ and the third muon. The latter implicitly includes the $b \to \mu X$ branching fraction for the third muon. Depending on the particular $\Delta\phi$ bin, an accuracy of 15-25% on the differential cross-section can be obtained, combining statistical and systematic uncertainty. An accuracy at the 10% level is expected for the integrated total cross section. We obtain, in $50\,\mathrm{pb}^{-1}$, $\sigma(pp \to b\bar{b}X) = 451 \pm 50\ \mu$b, to be compared to the generated value of 438 μb in PYTHIA. It is clear from Fig. 8 that a measurement is possible with as little as $50\,\mathrm{pb}^{-1}$, which should be available in the first physics run at the LHC.

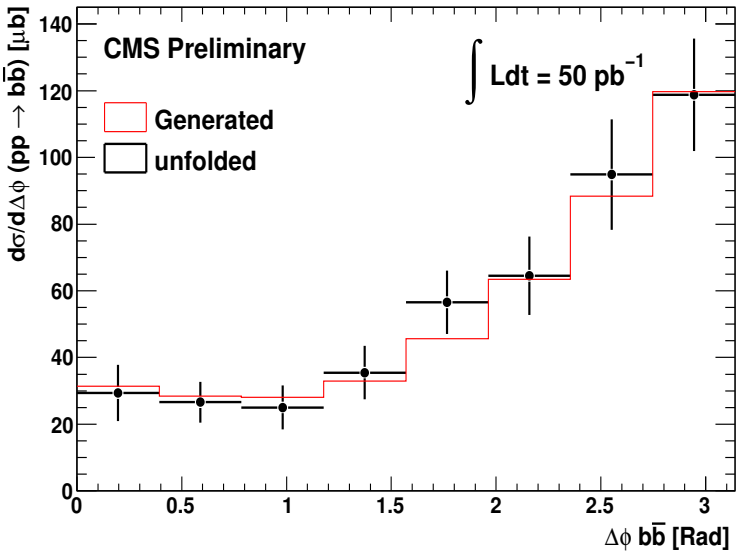

Figure 8: Final differential cross section measurement $d\sigma/d\Delta\phi$ after unfolding and including systematic uncertainties.

A Additional Plots

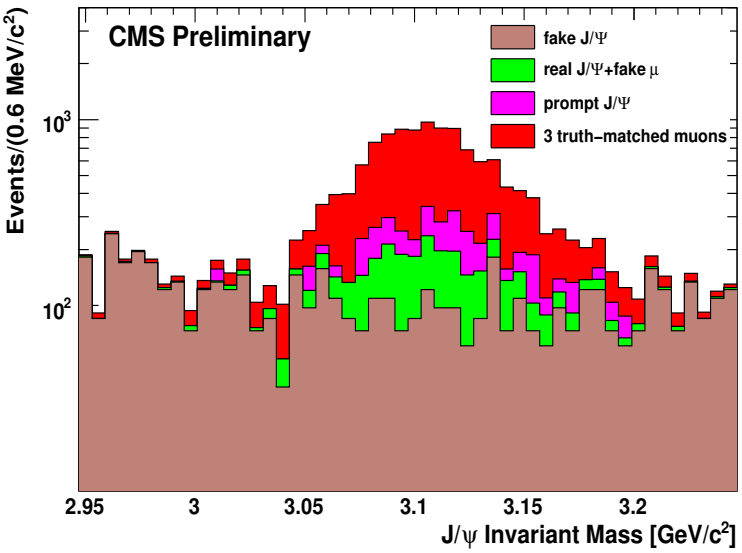

Figure 9: J/ψ invariant mass distribution in logarithmic scale after all the selection criteria. The different truth-matched components are stacked and shown in different colors.

References

[1] M. Mangano, P. Nason, and G. Ridolfi, Nucl. Phys. B**373**, 295 (1992).

[2] D. E. Acosta *et al.* [CDF Collaboration], Phys. Rev. D**71**, 092001 (2005), and references therein.

[3] M. Cacciari, and P. Nason, Phys. Rev. Lett. **89**, 122003 (2002).

[4] F. Halzen, W. Y. Keung, and D. M. Scott, Phys. Rev. D**27**, 1631 (1983).

[5] E. L. Berger, *et al.*, Phys. Rev. Lett. **86**, 4231 (2001).

[6] T. Aaltonen *et al.* [CDF Collaboration], Phys. Rev. D **77**, 072004 (2008); T. Aaltonen *et al.* [CDF Collaboration], arXiv:0810.5357 (2008).

[7] T. Sjostrand and M. Bengtsson, Comput. Phys. Comm. **43**, 367 (1987); H.-U. Bengtsson and T. Sjostrand, Comput. Phys. Comm. **46**, 43 (1987).

[8] D J. Lange, Nucl. Instrum. Methods Phys. Res., Sect. A**462**, 152 (2001).

[9] The CMS Collaboration, "The Trigger and Data Acquisition Project", Vol. II, CERN/LHCC 2002-026; "CMS High Level Trigger", CERN/LHCC 2007-021.

[10] C. Amsler *et al.* [Particle Data Group], Phys. Letters B**667**, 1 (2008).

[11] A. Hocker and V. Kartvelishvili, Nucl. Instrum. Meth. A**372**, 469 (1996).

[12] A. Abulencia *et al.* [CDF Collaboration], Phys. Rev. Lett. **99**, 132001 (2007).

[13] B. Aubert *et al.* [BaBar Collaboration], Phys. Rev. D**67**, 032002 (2003).